Boise State University

ScholarWorks

Comparing Aerial Lidar Observations with Terrestrial Lidar and Snow-Probe Transects from NASA's 2017 SnowEx Campaign

Zach Uhlmann
Boise State University

Lucas Spaete
Boise State University

Nancy F. Glenn
Boise State University, nancyglenn@boisestate.edu

Key Points:
- Snow depth magnitude and spatial variability derived from aerial lidar generally agreed with terrestrial lidar and snow-probe transects
- Snow depth differences between aerial and terrestrial lidar underneath the canopy were comparable to differences in the open
- Largest differences between aerial and terrestrial lidar were in areas with shrubs and where terrestrial lidar incidence angles were high

Supporting Information:
- Supporting Information S1

Correspondence to:
W. R. Currier,
currierw@uw.edu

Comparing Aerial Lidar Observations With Terrestrial Lidar and Snow-Probe Transects From NASA's 2017 SnowEx Campaign

William Ryan Currier[1] [iD], Justin Pflug[1] [iD], Giulia Mazzotti[2] [iD], Tobias Jonas[2], Jeffrey S. Deems[3,4] [iD], Kat J. Bormann[5] [iD], Thomas H. Painter[5] [iD], Christopher A. Hiemstra[6], Arthur Gelvin[6], Zach Uhlmann[7], Lucas Spaete[7], Nancy F. Glenn[7] [iD], and Jessica D. Lundquist[1] [iD]

[1]Department of Civil and Environmental Engineering, University of Washington, Seattle, WA, USA, [2]WSL Institute for Snow and Avalanche Research SLF, Davos Dorf, Switzerland, [3]Cooperative Institute for Research in the Environmental Sciences, University of Colorado Boulder, Boulder, CO, USA, [4]National Snow and Ice Data Center, Boulder, CO, USA, [5]Jet Propulsion Laboratory, California Institute of Technology, Pasadena, CA, USA, [6]Cold Regions Research and Engineering Laboratory, Fort Wainwright, AK, USA, [7]Department of Geosciences, Boise State University, Boise, ID, USA

Abstract NASA's 2017 SnowEx field campaign at Grand Mesa, CO, generated Airborne Laser Scans (ALS), Terrestrial Laser Scans (TLS), and snow-probe transects, which allowed for a comparison between snow depth measurement techniques. At six locations, comparisons between gridded ALS and TLS observations, at 1-m resolution, had a median snow depth difference of 5 cm, root-mean-square difference of 16 cm, mean-absolute difference of 10 cm, and 3-cm difference in standard deviation. ALS generally had greater but similar snow depth values to TLS, and results were not sensitive to the gridded cell size between 0.5 and 5 m. The greatest disagreements were where snow-off TLS scans had shrubs and high incidence angles, leading to deeper snow depths (>10 cm) from ALS than TLS. The low vegetation and oblique angles caused occlusion in the TLS data and thus produced higher snow-off bare Earth models relative to the ALS. Furthermore, in subcanopy areas where both ALS and TLS data existed, snow depth differences were comparable to differences in the open. Meanwhile, median values from 52 snow-probe transects and near-coincident ALS data had a mean difference of 6 cm, root-mean-square difference of 8 cm, mean-absolute difference of 7 cm, and a mean difference in the standard deviation of 1 cm. Snow depth probes had greater but similar snow depth values to ALS. Therefore, based on comparisons with TLS and snow depth probes, ALS captured snow depth magnitude with better than or equal agreement to what has been reported in previous studies and showed the ability to capture high-resolution spatial variability.

1. Introduction

Previous snow depth spatial variability studies have benefited from advancements in airborne and terrestrial lidar systems, which are capable of producing high-resolution (<5 m) snow depth maps (Broxton et al., 2015; Currier & Lundquist, 2018; Deems et al., 2006, 2008, 2013, 2015; Grünewald et al., 2010; Hedrick et al., 2018; Mott et al., 2010; Painter et al., 2016; Revuelto et al., 2015; Schirmer et al., 2011; Schirmer & Lehning, 2011; Trujillo et al., 2007, 2009; Wayand et al., 2018). Uncertainties in Airborne Laser Scanning (ALS) are a function of the laser's range, the topography, and the accuracy and precision of the laser's geospatial positioning and orientation (Deems et al., 2013; Glennie, 2007). Terrestrial Laser Scanning (TLS) views the terrain from a fixed height and position, and has similar sources of uncertainty to ALS (Figure 1). A stable ground surface is necessary to minimize error in TLS data collections, and surveys that take place in deep snow can be subjected to snow compaction throughout the scan (Deems et al., 2015; Hartzell et al., 2015).

The scan angle of an ALS or TLS survey is important to consider because the laser beam diverges as the range increases, which can increase the snow depth uncertainty, specifically in areas where the laser has a high incidence angle (Deems et al., 2013; Hartzell et al., 2015). For instance, as the incidence angle increases, the footprint of an obliquely incident laser pulse elongates when interacting with the surface, which introduces uncertainty in the return signal. A rigorous error propagation effort showed that discrete lidar returns with incidence angles greater than 60° at a 500-m range have an additional vertical and horizontal uncertainty introduced, which ranges from 2–10 cm (Hartzell et al., 2015). This uncertainty will rise in
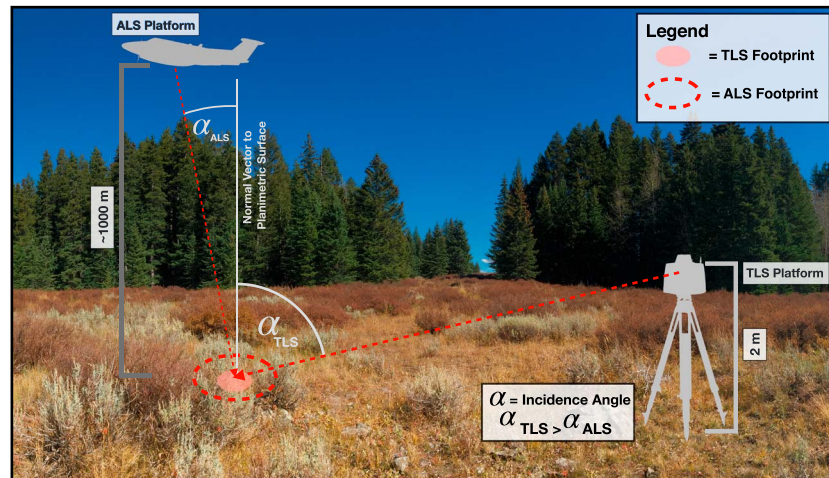
Figure 1. Conceptual diagram of ALS and TLS scans during the snow-off survey. Photo is from the western end of Grand Mesa, CO, USA. Aircraft height and size are not to scale. ALS = Airborne Laser Scans; TLS = Terrestrial Laser Scans.

regions where vegetation cover occludes (or partially occludes) the laser from penetrating to the ground (Anderson et al., 2018).

These sources of uncertainty, however, are offset by the ability of lidar systems to map snow depth at high resolutions across complex and forested terrain. Therefore, airborne lidar has been used to map snow depth since 2001 (Hopkinson et al., 2001, 2004). Since then, snow depth maps derived from ALS and TLS have been compared with snow-probe measurements, Global Navigation Satellite System (GNSS) observations, and acoustic snow depth sensors (Table 1). These studies have used a collection of point-scale measurements, characterized by a small support of 0.01–0.5 m (Blöschl, 1999), which can contain geolocation uncertainty and do not provide the same measurement density over wide areas as lidar scans. Therefore, previous studies were unable to explicitly quantify the ability for aerial or terrestrial lidar systems to determine the spatial variability of snow depth. Furthermore, these studies come to different conclusions as to whether errors are higher in the forest or in the open, and whether these errors are due to low-lying vegetation or significant geolocation errors (Hopkinson et al., 2004; Reutebuch et al., 2003; Tinkham et al., 2014). Lastly, previous studies have not explicitly evaluated discrepancies in lidar data due to different viewing perspectives.

NASA's 2017 SnowEx field campaign at Grand Mesa, CO, generated a suite of coincident, or nearly coincident, airborne, and ground-based observations—including ALS, TLS, and snow depth probe transects. This extensive data set offers the unique opportunity to test the consistency of different snow depth measuring techniques and test their sensitivity at various spatial resolutions over a gradient of different vegetation types (Kim, 2018; Kim et al., 2017).

In this technical note, we comprehensively compare ALS observations to TLS surveys for the first time and also compare ALS observations to snow-probe transects from NASA's 2017 SnowEx campaign. We therefore quantify the sensitivity and consistency of different snow depth measurement techniques to capture spatial variability at high spatial resolution across various land cover types, including directly underneath the forest canopy.

2. Location and Data

2.1. Grand Mesa, CO

NASA's 2017 SnowEx campaign took place on Grand Mesa in western Colorado, USA (Figure 2). There were six TLS sites with variable components of grasses, shrubs, and trees. Shrubby cinquefoil (*Dasiphora fruticosa*), big sagebrush (*Artemesia tridentata* ssp. *vaseyena*), and silver sagebrush (*A. cana* ssp. *viscidula*) are all under 1-m height and prevalent on the windier western end of the Mesa. Forests were present at four TLS sites (A, K, N, and the Ranger Station) and are predominantly Engelmann spruce (*Picea engelmannii*), with much rarer components of subalpine fir (*Abies lasiocarpa*), Aspen (*Populus tremuloides*), and lodgepole

Table 1
Previous Evaluations of Aerial and Terrestrial Lidar

Study	Laser	ALS/TLS	Snow (Y/N)	Height above terrain (m)	Evaluation method	Evaluation summary
Reutebuch et al. (2003)	Saab TopEye Lidar System (Helicopter)	ALS	N	200	GNSS	Different forest densities: (Mean difference ±1σ) Clearcut: 0.16 ± 0.23 m, Heavily thinned: 0.18 ± 0.14 m; Lightly thinned: 0.18 ± 0.18m; Uncut: 0.31 ± 0.29 m
Hopkinson et al. (2001, 2004)	Optech ALTM 1210 and 1225	ALS	Y	700–750	Snow depth probes	Mean difference: 0.01–0.13 m; canopy understory can systematically underestimate snow depth
Hopkinson et al. (2005)	Optech ALTM 2050	ALS	N	1,200	GNSS	Mean difference: 0.04 m
Prokop et al. (2008)	Riegl LPM-i800HA	TLS	Y	~2	Tachymetry and snow probing	Tachymetry: $1\sigma = 0.02$ m Snow probe: $1\sigma = 0.1$ m
Prokop (2008)	Riegl LPM-i800HA and LPM-2K	TLS	Y	~2	Snow depth probes	Snow depth accuracy within 0.1 m for distances <500 m
DeBeer and Pomeroy (2010)	Optech ALTM 3100	ALS	Y	3,500	Snow depth Probes	RMSD was 0.17 m; greater error of up to 0.6 m in locations with exposed alpine shrubs.
Spaete et al. (2011)	Leica ALS50 Phase II	ALS	N	900	GNSS	RMSD 0.07–0.22 m – largest errors on herbaceous slopes
Tinkham et al. (2011)	Leica ALS50 Phase II	ALS	N	900	GNSS	RMSD 0.13–0.46 m depending on vegetation type. Mean RMSD: 0.28 m
Hopkinson et al. (2012)	Optech ALTM 3100	ALS	Y	3,500	Snow depth probes	Mean differences: lower open area: 0.07 m; forested areas: 0.13 m; Alpine open area: −0.04 m; lidar generally had higher snow depth than snow probe
Tinkham et al. (2014)	Leica ALS50 Phase II	ALS	Y	900	Snow depth probes	Shrub/meadow: RMSD = 0.14 m; forested areas 0.2–0.35 m
Kirchner et al. (2014)	Optech GEMINI ALTM 1233	ALS	Y	600	Plowed area comparison	Biased up to 0.05 m
Harpold et al. (2014)	Optech GEMINI ALTM 1233	ALS	Y	Varied	Acoustic snow depth Sensors	RMSD 0.23 m between 60 acoustic snow depth sensors
Deems et al. (2015)	Riegl VZ-4000 and Riegl VZ-6000	TLS	Y	~2	Snow pit	Difference was 0.01 m between TLS and corner of snow pit
Painter et al. (2016)	Riegl Q1560 - Dual lasers.	ALS	Y	~3,000	Snow depth probes	Exposed area; mean absolute difference: 0.08 m in 15 × 15-m area

Note. ALS = Airborne Laser Scans; TLS = Terrestrial Laser Scans; RMSD = root-mean-square difference; GNSS = Global Navigation Satellite System.

pine (*Pinus contorta* var. *latifolia*). The Ranger Station site was unique in that it included a grassy picnic area, parking lot, and two cabins with partly snow-free roofs.

2.2. ALS

The snow-off ALS survey was collected by the NASA Airborne Snow Observatory (ASO) on 26 September 2016, with snow-on data collected on 8 and 16 February 2017 using methods, instrumentation, and processing steps described in Painter et al. (2016) to receive three-dimensional point cloud data. All three flight altitudes were around 4,100 m above sea level, which is about 1,000–1,100 m above the terrain leading to a footprint size of about 26 cm and an average total point density of around 18 points per square meter. See Text S1a in the supporting information for additional details.

2.3. TLS

Snow-off TLS data were collected between 26 September and 2 October 2016 using two different lidar scanners, a Riegl VZ-1000 and Leica C-10 ScanStation (Table S1). Snow-on scans were collected on near-coincident dates in February (Table S1), and tripod legs were placed in contact with the ground or a packed snow surface to minimize potential errors from snow compaction throughout the survey. Scans with the
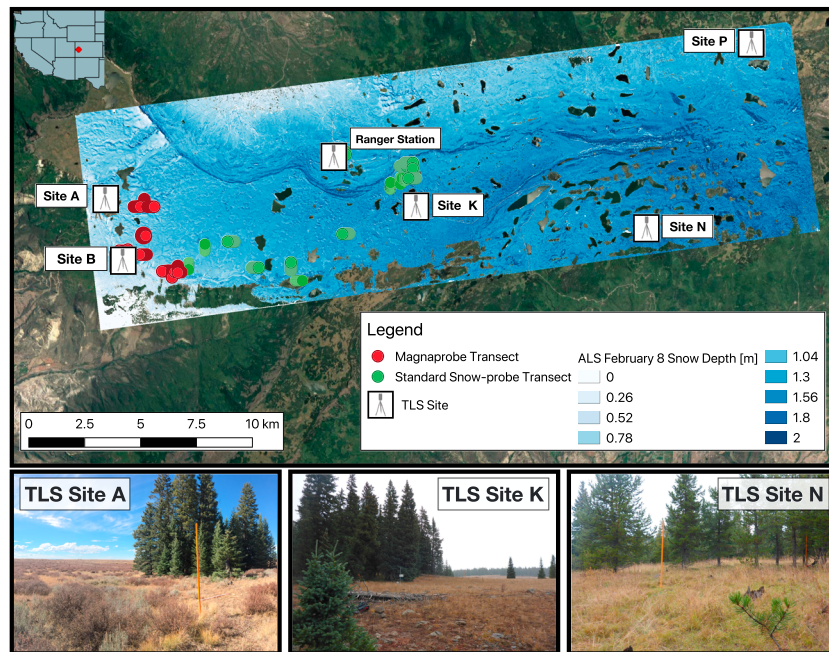
Figure 2. Distribution of ALS, TLS, and snow-probe transects across Grand Mesa, Colorado (top panel). Ground images collected in September 2016 demonstrate the variability and state of the ground vegetation at the TLS sites (bottom panels). Many gaps within the ALS data are water bodies, which were intentionally masked out with the national hydrography data set. ALS = Airborne Laser Scans; TLS = Terrestrial Laser Scans.

Riegl VZ-1000 were obtained from 50° off-nadir, to 150° pointing upward, in a 360° rotation at a 0.03° increment (angular resolution of 0.03°) in both rotation planes. Scans with the Leica C-10 ScanStation were obtained from 45° off-nadir, to 180° pointing upward, in a 360° rotation at a 0.06° increment in both rotation planes. See Text S1b for additional details.

2.4. Snow Depth Probe Transects

Both a standard 3-m snow depth probe and a 1.2-m GPS-equipped Magnaprobe (Sturm & Holmgren, 2018), which automatically records the geolocation of each snow depth measurement to within ± 2.5 m, were used to compare with ALS data. Snow-probe transects did not overlap with TLS surveys; therefore, only ALS was compared with snow-probe transects. The snow depth measurement uncertainty of both snow depth probe measurements is estimated to be around ± 5 cm due to the potential penetration of the probe's tip into the soil underneath the snow, impacts of low vegetation, and the angle of the probe (Sturm & Holmgren, 2018). The location of each standard snow-probe transect was estimated using linear lines between georeferenced transect poles used to guide surveyors from beginning to end. This resulted in an estimated ± 5-m geolocation error for each snow depth measurement. More details are provided in Text S2.

3. Methods

3.1. Classification and Gridding

Three-dimensional point clouds were classified as ground and nonground points (e.g., vegetation) using LAStools *lasground* (http://rapidlasso.com/lastools/), which is a variation of the Axelsson (2000) methodology. We used default parameters within *lasground,* with the exception of choosing step sizes of 2 and 10 m to allow for some uncertainty in the classification.

Snow-on and snow-off scans from both ALS and TLS were gridded to 0.5-, 1-, 2-, 3-, and 5-m spatial resolutions using two strategies: first, using the lowest of all ground points within each grid cell, and second, averaging all ground-classified points within a grid cell. With both strategies, if the difference between the two elevation models built with the two different classifications (step 2 m and 10 m) was greater than 20 cm,

Table 2
Percentage of the Domain That Contained a Vegetation Height >2 m (Forest), Snow Depth Differences Between Lidar Data Sets at 1-m Spatial Resolution in the Open and in the Forest, and Percent of the Forested Area Where Both ALS and TLS Data Were Unable to Derive Snow Depth

	Forested area	Median difference (Open/Forest) median(ALS − TLS)	RMSD (Open/Forest) $\sqrt{\frac{\sum(ALS-TLS)^2}{N}}$	Mean absolute difference (Open/Forest) $\overline{abs}(ALS-TLS)$	Difference in standard deviation (Open/Forest) $\sigma_{ALS} - \sigma_{TLS}$	Forested area missing by ALS	Forested area missing by TLS	Forested area captured by both ALS and TLS
Site A	17% 2,685 m^2	2 cm 0 cm	17 cm 18 cm	12 cm 11 cm	−3 cm −3 cm	26% 689 m^2	15% 405 m^2	63% 1,687 m^2
Site B	—	1 cm —	16 cm —	10 cm —	−7 cm —	—	—	—
Site K	20% 3,552 m^2	4 cm 5 cm	9 cm 13 cm	7 cm 10 cm	−1 cm −4 cm	12% 417 m^2	24% 859 m^2	67% 2,392 m^2
Ranger Station	36% 2,257 m^2	12 cm 16 cm	25 cm 34 cm	18 cm 24 cm	−6 cm −6 cm	21% 479 m^2	30% 684 m^2	59% 1,328 m^2
Site P	—	7 cm —	11 cm —	8 cm —	6 cm —	—	—	—
Site N	37% 3,887 m^2	6 cm 8 cm	20 cm 22 cm	12 cm 15 cm	−5 cm −5 cm	14% 549 m^2	17% 663 m^2	71% 2,745 m^2
All forested sites	24% 12,381 m^2	5 cm 6 cm	16 cm 22 cm	10 cm 14 cm	−3 cm −3 cm	17% 2,134 m^2	21% 2,611 m^2	66% 8,152 m^2
All sites (Forest + Open)	—	5 cm	16 cm	10 cm	−3 cm	—	—	—

Note. ALS = Airborne Laser Scans; TLS = Terrestrial Laser Scans; RMSD = root-mean-square difference.

then that grid cell was removed from the comparison. Across all sites, this filtering removed 0.14% of the snow depth values. Lastly, while there was little difference in the results based on gridding methodology, we focus our results on snow depth values derived from the lowest-return gridding method and show results from the alternative strategy in the supporting information (Text S4).

3.2. TLS Incidence Angle

For each TLS site, we used the geographic position of the snow-off TLS scan position, the ALS digital terrain model at 1-m resolution, and the TLS scanner's Height Relative to the Target Terrain Height (HRTTH) to derive an incidence angle map for each snow-off TLS scan position. From each scan position, we searched out radially, computing the distance between the TLS scanner and the target grid cell (DIST). We then approximated the slope of each target grid cell using the two adjacent elevation values within the azimuthal direction of the search line. The incidence angles (θ) corresponding to each snow-off scan position were computed over the entire domain (equation (1)) to create a set of incidence angle maps for each snow-off TLS scan position. Finally, the lowest incidence angle within the set of maps was determined for each grid cell.

$$\theta = \tan^{-1}\left(\frac{DIST}{HRTTH}\right) - slope \tag{1}$$

4. Results

4.1. ALS Versus TLS Comparison

Both ALS and TLS surveys captured a similar snow depth magnitude and variability. Using all data where the 1-m ALS and TLS snow depth grids overlapped, we found a median difference of 5 cm (4%), root-mean-square difference (RMSD) of 16 cm, and mean absolute difference of 10 cm (Table 2). At individual TLS sites, ALS and TLS snow depth differences ranged from a 1–13 cm (1–10%) median difference (Figures 3 and S3 and Tables 2 and S3), 10- to 28-cm RMSD (Table S5), and a 7- to 20-cm mean absolute difference (Table S6), where the ALS data generally showed deeper snow depth values. The closest agreement occurred at TLS Sites A, B, and K, where median snow depth differences were less than 5 cm, while the worst agreement was at the Ranger Station, where median snow depth difference was 13 cm.
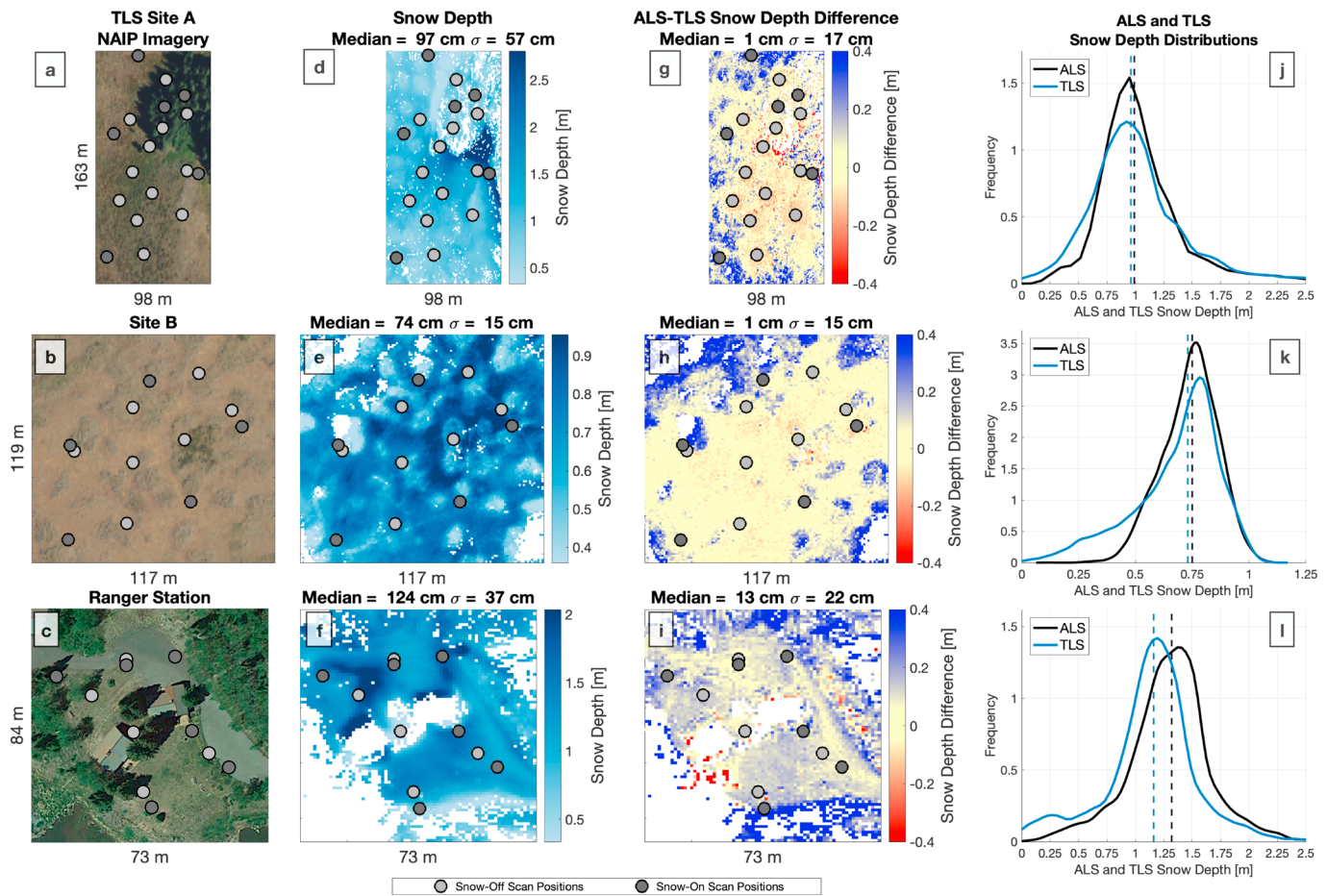
Figure 3. (a–c) True color imagery for Terrestrial Laser Scans (TLS) Sites A, B (USDA NAIP), and the Ranger Station (© 2018 Google). (d–f) Average of the Airborne Laser Scans (ALS) and TLS snow depth. Areas that were missing either ALS or TLS data were removed from the analysis and are shown in white. (g–i) ALS snow depth minus TLS snow depth at 1-m resolution. (j–l) ALS and TLS snow depth distributions. Dashed lines show the median value of the distribution. Figure S3 shows similar results for TLS Site K, N, and P.

At individual sites, the difference in standard deviations from the 1-m resolution ALS and TLS snow depth ranged between −7 and 1 cm (mean: −3 cm). The TLS snow depth data generally contained a higher standard deviation due to the difficulty in obtaining a snow-off surface while scanning shrubs at a high-incidence angle (section 5.1.1). Snow-off or snow-on surfaces were not compared directly because the ALS data were not subjected to absolute registration, resulting in a vertical bias relative to the TLS snow-off data (Text S1).

Differences in the median snow depth values between ALS and TLS were generally not sensitive to the gridding resolution between 50 cm and 5 m (Table S3). However, at the Ranger Station, differences in median snow depth values increased 5 cm as the gridding resolution increased from 50 cm to 5 m. Similar to median snow depth differences, the difference in standard deviations between ALS and TLS were generally not sensitive to the gridding resolution, except at the Ranger Station and Site P (Table S4).

4.2. ALS Versus Snow-Probe Transects

In general, both standard and magnaprobe snow depth measurements had higher snow depths than the ALS snow depth values on both 8 and 16 February (Figure 4). The median values from combining both standard and magnaprobe snow depth transects were on average 6-cm greater than the median values from ALS on 8 and 16 February, and the mean absolute difference and RMSD of that comparison were 7 and 8 cm, respectively.

On average, snow-probe transects agreed with the ALS standard deviation. For instance, ALS and snow-probe transects differed in their standard deviations by 1 and 0 cm on 8 and 16 February,
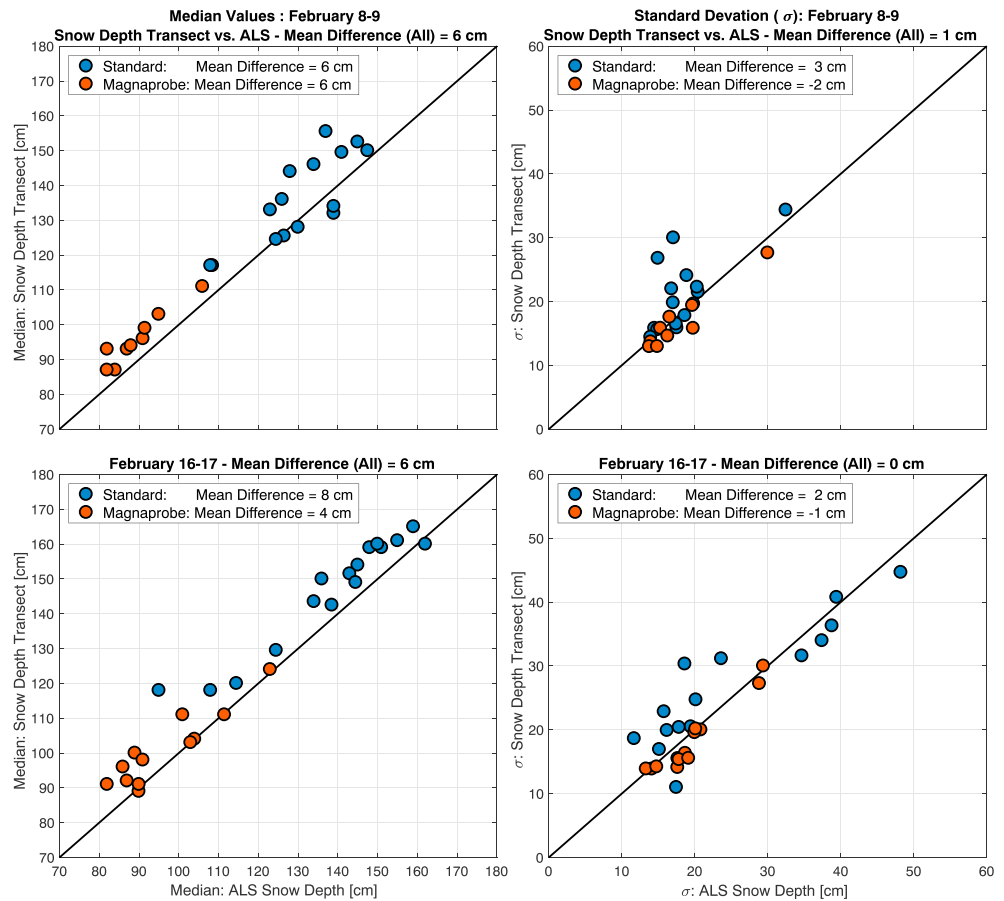
Figure 4. (left column) Comparison between median snow depth values from snow-probe transects (standard and magnaprobe) and ALS snow depth data from 8 and 16 February 2017. (right column) Comparison between standard deviations from the snow-probe transects (standard and magnaprobe) and the ALS data from 8 and 16 February 2017. "(All)" implies that the mean difference was used by combining either the standard deviation of the transect or the median snow depth values from both the standard and magnaprobe snow depth transects. ALS = Airborne Laser Scans.

respectively. The mean absolute difference and RMSD between the standard deviation values from the snow-probe and ALS transects were 3 and 4 cm, respectively, on both 8 and 16 February. The general agreement between ALS and TLS standard deviations, as well as between standard deviations from ALS and snow depth transects, suggests that ALS data were able to resolve the snow depth variability at high spatial resolution.

4.3. ALS and TLS Vegetation Interactions

At TLS Sites A, K, N, and the Ranger Station, the domains were partly forested (Table 2). At these locations, the median snow depth difference between ALS and TLS was 1 cm greater underneath the canopy than in the open. Similarly, the RMSD and mean absolute difference between ALS and TLS snow depth increased by 6 and 4 cm, respectively. The largest change in RMSD and mean absolute difference was at the Ranger Station site, which generally performed worse than the other sites likely due to multipath errors (see section 5.1.2). Removing the Ranger Station site, the RMSD and mean absolute difference only increased by 3 and 2 cm. Lastly, the difference in the snow depth's standard deviation between ALS and TLS did not generally increase (Table 2). This implied that ALS snow depth data were not adversely affected by canopy cover. However, between the four forested sites, ALS data were missing 17% of the 1-m grid cells, and TLS data were missing 21%. This left 66% of the total forested area to compare ALS and TLS snow depth (Table 2).

5. Discussion

5.1. Sources of Snow Depth Differences

5.1.1. Shrubs and High Incidence Angles

Despite similar differences between ALS and TLS within open and forested areas, TLS snow depth was 10- to 13-cm less than ALS snow depth in areas where shrub heights were greater than 20 cm in combination with TLS incidence angles that were higher than 80° (Figure S5). These localized differences caused the TLS derived snow depth to be more heterogenous and have lower median snow depths than ALS data (Tables 2 and S4).

These differences were likely due to the different viewing perspectives of ALS and TLS (Figure 1). For instance, it is easier to penetrate a shrub with a laser at a normal rather than an oblique angle. Prior studies using snow depth probes or GNSS observations noted that airborne lidar systematically underestimated snow depth in areas with significant ground vegetation (Hopkinson et al., 2004), or ALS errors increased where there were shrubs (DeBeer & Pomeroy, 2010; Spaete et al., 2011). In contrast, our results suggested that aerial lidar did penetrate at least partly through the shrubs, while the terrestrial lidar was partially occluded by the shrubs (Anderson et al., 2018), ultimately biasing the TLS-derived snow depth too low. The ability for ALS to see through the shrubs in our study is likely explained by differences in ground vegetation type between Grand Mesa and previous studies, the relatively low altitude and high point density of the ALS survey, and the development in recent years of more advanced algorithms that extract discrete lidar returns from the return energy waveforms (Pfennigbauer & Ullrich, 2011; Ullrich & Pfennigbauer, 2011).

5.1.2. Multipath Errors

A combination of high incidence angles and shrubs was unable to explain all of the snow depth differences. For instance, we still found greater than 10-cm snow depth differences near the TLS snow-off scan positions at the Ranger Station site. At the Ranger Station site, TLS scans were not vertically or horizontally registered with each other as a result of multipath errors in the GNSS measurements. Multipath errors were likely more significant at the Ranger Station than in other TLS sites due to the topography, buildings, and vegetation. We were unable to quantify potential registration errors at other sites due to the lack of a snow-free static structure; however, qualitative point cloud comparisons with trees showed that the ALS and TLS surveys were coregistered with each other. Fortunately, we were able to detect and correct for these multipath errors at the Ranger Station site. Registering both the TLS scans to the snow-free roof in the ALS data improved the metrics at the Ranger Station site. However, the Ranger Station site was a smaller domain compared to other TLS sites; therefore, the TLS registration only changed the median snow depth difference using all ALS and TLS snow depth data from 5 to 4 cm. Furthermore, there was little change in other metrics using all the ALS and TLS snow depth (Table S11).

5.1.3. Snow Depth Probes

ALS-derived snow depth was 6 cm less on average than what was recorded with snow-probe measurements. We suspect that the general bias in ALS measurements relative to snow-probe measurements is due to snow-probe penetration through the soil/vegetation (Sturm & Holmgren, 2018). For instance, human observers are more likely to press a probe into duff or soft ground, and are known to unintentionally avoid making measurements in very low or zero snow (both of which would bias probe measurements high). Furthermore, while ALS reached the ground through shrubs more than TLS, it may have done so less frequently than a human observer. Interestingly, both magnaprobe and standard snow depth transects generally showed higher snow depth values despite different methodologies. For instance, magnaprobe geolocation uncertainties are independent between each measurement, while the geolocation uncertainty of a standard snow-probe transect increases along the transect line. Since both types of snow-probe transects typically provided higher median snow depth values than ALS, snow depth differences between median values were not likely due to geolocation errors.

5.2. Comparisons to Previous Studies

Despite contrasting median snow depth differences between ALS versus TLS and ALS versus snow-probe transects, the RMSD was 16 cm between all 1-m gridded ALS and TLS snow depth data. Meanwhile, the RMSD between median values from ALS and snow-probe transects was 8 cm. This suggested that ALS data, which were evaluated using TLS data and 52 snow-probe transects ($n = 10,926$) through a variety of vegetation, resulted in a RMSD that was equal to or better than previous studies which evaluated ALS using point

based measurements (DeBeer & Pomeroy, 2010; Harpold et al., 2014; Spaete et al., 2011; Tinkham et al., 2011, 2014). Lastly, the mean absolute difference using all ALS and TLS data was 10 cm, while the mean absolute difference between the median values of the ALS and snow-probe transects was 7 cm. These mean absolute differences were similar or less than the mean absolute difference reported in Painter et al. (2016); (Table 1).

5.3. Context of the Snow Depth Differences

After coregistering the Ranger Station site (section 5.1.2.), the median snow depth differences were relatively small, ranging between 1 and 7 cm, or 1–5% using the observed median snow depth across all TLS sites (1.29 m). Because the differences in observations are absolute in nature, as the snow depth decreases, the percent differences will increase. For instance, if the median snow depth was 25 cm, the percent difference in median values would have ranged from 4–28%.

6. Conclusions

Both ALS and TLS data captured a similar spatial variability and magnitude of snow depth at high spatial resolutions. For instance, at 1-m resolution, ALS and TLS data had a median difference of 5 cm, RMSD of 16 cm, a mean absolute difference of 10 cm, and a difference in standard deviation of 3 cm. Additionally, comparisons between median values from ALS and snow-probe transects showed a mean difference of 6 cm, mean absolute difference of 7 cm, RMSD of 8 cm, and a mean difference in the standard deviation of 1 cm. These differences, in combination with the differences between ALS and TLS were similar or better than those reported in previous evaluations of ALS.

In addition, ALS and TLS showed similar differences underneath the canopy to those in the open, but ALS data at 1-m spatial resolution were unable to derive snow depth in part of the forested area due to missing ground returns. Furthermore, ALS and TLS both inherently have different viewing perspectives. In localized areas where the snow-off TLS scans had high incidence angles and were scanning shrubs, TLS surveys derived shallower snow depths relative to ALS. This implied that ALS pulses were more likely to be from the ground, whereas the ground was relatively more occluded in the TLS data. Using these results, we provide suggestions for future campaigns that evaluate ALS data (Text S5). These recommendations focus on explicitly evaluating void filling routines in forested areas (Zheng et al., 2016), minimizing differences in viewing perspective, and ground controlling observations to provide absolute georegistration.

References

Anderson, K. E., Glenn, N. F., Spaete, L. P., Shinneman, D. J., Pilliod, D. S., Arkle, R. S., et al. (2018). Estimating vegetation biomass and cover across large plots in shrub and grass dominated drylands using terrestrial lidar and machine learning. *Ecological Indicators*, *84*(October 2017), 793–802. https://doi.org/10.1016/j.ecolind.2017.09.034

Axelsson, P. (2000). DEM generation from laser scanner data using adaptive TIN models. *International Archives of Photogrammetry and Remote Sensing*, *60*(2), 71–80. https://doi.org/10.1016/j.isprsjprs.2005.10.005

Blöschl, G. (1999). Scaling issues in snow hydrology. *Hydrological Processes*, *13*(14–15), 2149–2175. https://doi.org/10.1002/(SICI)1099-1085(199910)13:14/15<2149::AID-HYP847>3.0.CO;2-8

Broxton, P. D., Harpold, A. A., Biederman, J. A., Troch, P. A., Molotch, N. P., & Brooks, P. D. (2015). Quantifying the effects of vegetation structure on snow accumulation and ablation in mixed-conifer forests. *Ecohydrology*, *8*(6), 1073–1094. https://doi.org/10.1002/eco.1565

Currier, W. R., & Lundquist, J. D. (2018). Snow depth variability at the forest edge in multiple climates in the Western United States. *Water Resources Research*, *54*, 8756–8773. https://doi.org/10.1029/2018WR022553

DeBeer, C. M., & Pomeroy, J. W. (2010). Simulation of the snowmelt runoff contributing area in a small alpine basin. *Hydrology and Earth System Sciences*, *14*(7), 1205–1219. https://doi.org/10.5194/hess-14-1205-2010

Deems, J. S., Fassnacht, S. R., & Elder, K. J. (2006). Fractal distribution of snow depth from lidar data. *Journal of Hydrometeorology*, *7*(2), 285–297. https://doi.org/10.1175/JHM487.1

Deems, J. S., Fassnacht, S. R., & Elder, K. J. (2008). Interannual consistency in fractal snow depth patterns at two Colorado mountain sites. *Journal of Hydrometeorology*, *9*(5), 977–988. https://doi.org/10.1175/2008JHM901.1

Deems, J. S., Gadomski, P. J., Vellone, D., Evanczyk, R., LeWinter, A. L., Birkeland, K. W., & Finnegan, D. C. (2015). Mapping starting zone snow depth with a ground-based lidar to assist avalanche control and forecasting. *Cold Regions Science and Technology*, *120*, 197–204. https://doi.org/10.1016/j.coldregions.2015.09.002

Deems, J. S., Painter, T. H., & Finnegan, D. C. (2013). Lidar measurement of snow depth: A review. *Journal of Glaciology*, *59*(215), 467–479. https://doi.org/10.3189/2013JoG12J154

Glennie, C. (2007). Rigorous 3D error analysis of kinematic scanning LIDAR systems. *Journal of Applied Geodesy*, *1*(3), 147–157. https://doi.org/10.1515/jag.2007.017

Grünewald, T., Schirmer, M., Mott, R., & Lehning, M. (2010). Spatial and temporal variability of snow depth and ablation rates in a small mountain catchment. *Cryosphere*, *4*(2), 215–225. https://doi.org/10.5194/tc-4-215-2010

Harpold, A. A., Guo, Q., Molotch, N., Brooks, P. D., Bales, R., Fernandez-Diaz, J. C., et al. (2014). LiDAR-derived snowpack data sets from mixed conifer forests accross the Western United States. *Water Resources Research*, *50*, 2749–2755. https://doi.org/10.1002/2013WR013935.Received

Hartzell, P. J., Gadomski, P. J., Glennie, C. L., Finnegan, D. C., & Deems, J. S. (2015). Rigorous error propagation for terrestrial laser scanning with application to snow volume uncertainty. *Journal of Glaciology*, *61*(230), 1147–1158. https://doi.org/10.3189/2015JoG15J031

Hedrick, A. R., Marks, D., Havens, S., Robertson, M., Johnson, M., Sandusky, M., et al. (2018). Direct insertion of NASA airborne snow observatory-derived snow depth time series into the iSnobal Energy Balance Snow model. *Water Resources Research*, *55*, 1296–1311. https://doi.org/10.1029/2018WR023400

Hopkinson, C., Chasmer, L. E., Sass, G., Creed, I. F., Sitar, M., Kalbfleisch, W., & Treitz, P. (2005). Vegetation class dependent errors in lidar ground elevation and canopy height estimates in a boreal wetland environment. *Canadian Journal of Remote Sensing*, *31*(2), 191–206. https://doi.org/10.5589/m05-007

Hopkinson, C., Pomeroy, J., Debeer, C., Ellis, C., & Anderson, A. (2012). Relationships between snowpack depth and primary LiDAR point cloud derivatives in a mountainous environment. *IAHS-AISH Publication*, (September 2010), 354–358. Retrieved from http://cat.inist.fr/?aModele=afficheN&cpsidt=27917455

Hopkinson, C., Sitar, M., Chasmer, L., Gynan, C., Agro, D., Enter, R., Foster, J., et al. (2001). Mapping the spatial distribution of snowpack depth beneath a variable forest canopy using airborne laser altimetry. Proceedings of the 58th Annual Eastern Snow Conference, 253–264. Retrieved from http://www.easternsnow.org/proceedings/2001/Hopkinson_2.pdf

Hopkinson, C., Sitar, M., Chasmer, L., & Treitz, P. (2004). Mapping snowpack depth beneath forest canopies using airborne lidar. *Photogrammetric Engineering & Remote Sensing*, *70*(3), 323–330. https://doi.org/10.14358/PERS.70.3.323

Kim, E. (2018). How can we find out how much snow is in the world? *Eos*, *99*(June), 2–7. https://doi.org/10.1029/2018EO099939

Kim, E., Gatebe, C., Hall, D., Newlin, J., Misakonis, A., Elder, K., et al. (2017). NASA's SnowEx campaign: Observing seasonal snow in a forested environment. In 2017 IEEE International Geoscience and Remote Sensing Symposium (IGARSS) (pp. 1388–1390). IEEE. https://doi.org/10.1109/IGARSS.2017.8127222

Kirchner, P. B., Bales, R. C., Molotch, N. P., Flanagan, J., & Guo, Q. (2014). LiDAR measurement of seasonal snow accumulation along an elevation gradient in the southern Sierra Nevada, California. *Hydrology and Earth System Sciences*, *18*(10), 4261–4275. https://doi.org/10.5194/hess-18-4261-2014

Mott, R., Schirmer, M., Bavay, M., Grünewald, T., & Lehning, M. (2010). Understanding snow-transport processes shaping the mountain snow-cover. *Cryosphere*, *4*(4), 545–559. https://doi.org/10.5194/tc-4-545-2010

Painter, T. H., Berisford, D. F., Boardman, J. W., Bormann, K. J., Deems, J. S., Gehrke, F., et al. (2016). The Airborne Snow Observatory: Fusion of scanning lidar, imaging spectrometer, and physically-based modeling for mapping snow water equivalent and snow albedo. *Remote Sensing of Environment*, *184*(July), 139–152. https://doi.org/10.1016/j.rse.2016.06.018

Pfennigbauer, M., & Ullrich, A. (2011). Improving quality of laser scanning data acquisition through calibrated amplitude and pulse deviation measurement. In Proceedings of SPIE (p. 76841F). Orlando. https://doi.org/10.1117/12.849641

Prokop, A. (2008). Assessing the applicability of terrestrial laser scanning for spatial snow depth measurements. *Cold Regions Science and Technology*, *54*(3), 155–163. https://doi.org/10.1016/j.coldregions.2008.07.002

Prokop, A., Schirmer, M., Rub, M., Lehning, M., & Stocker, M. (2008). A comparison of measurement methods: Terrestrial laser scanning, tachymetry and snow probing, for the determination of spatial snow depth distribution on slopes. *Annals of Glaciology*, *49*(1), 210–216. Retrieved from. http://id22079462.library.ingentaconnect.com/content/igsoc/agl/2008/00000049/00000001/art00034;jsessionid=14ehp1vm2wl3t.victoria, https://doi.org/10.3189/172756408787814726

Reutebuch, S. E., Mcgaughey, R. J., Andersen, H., & Carson, W. W. (2003). Accuracy of a high-resolution lidar terrain model under a conifer forest canopy. *Canadian Journal of Remote Sensing*, *29*(5), 527–535.

Revuelto, J., López-Moreno, J. I., Azorin-Molina, C., & Vicente-Serrano, S. M. (2015). Canopy influence on snow depth distribution in a pine stand determined from terrestrial laser data. *Water Resources Research*, *51*, 3476–3489. https://doi.org/10.1002/2014WR016496

Schirmer, M., & Lehning, M. (2011). Persistence in intra-annual snow depth distribution: 2. Fractal analysis of snow depth development. *Water Resources Research*, *47*, W09517. https://doi.org/10.1029/2010WR009429

Schirmer, M., Wirz, V., Clifton, A., & Lehning, M. (2011). Persistence in intra-annual snow depth distribution: 1. Measurements and topographic control. *Water Resources Research*, *47*, W09516. https://doi.org/10.1029/2010WR009426

Spaete, L., Glenn, N., Derryberry, D., Sankey, T., Mitchell, J., & Hardegree, S. (2011). Vegetation and slope effects on accutracy of LiDAR-derived DEM in the Sagebrush Steppe. *Remote Sensing Letters*, *2*(4), 317–326. https://doi.org/10.1080/01431161.2010.515267

Sturm, M., & Holmgren, J. (2018). An automatic snow depth probe for field validation campaigns. *Water Resources Research.*, *54*, 9695–9701. https://doi.org/10.1029/2018WR023559

Tinkham, W. T., Huang, H., Smith, A. M. S., Shrestha, R., Falkowski, M. J., Hudak, A. T., et al. (2011). A comparison of two open source LiDAR surface classification algorithms. *Remote Sensing*, *3*(3), 638–649. https://doi.org/10.3390/rs3030638

Tinkham, W. T., Smith, A. M. S., Marshall, H.-P., Link, T. E., Falkowski, M. J., & Winstral, A. H. (2014). Quantifying spatial distribution of snow depth errors from LiDAR using random forest. *Remote Sensing of Environment*, *141*, 105–115. https://doi.org/10.1016/j.rse.2013.10.021

Trujillo, E., Ramírez, J. A., & Elder, K. J. (2007). Topographic, meteorologic, and canopy controls on the scaling characteristics of the spatial distribution of snow depth fields. *Water Resources Research*, *43*, W07409. https://doi.org/10.1029/2006WR005317

Trujillo, E., Ramírez, J. A., & Elder, K. J. (2009). Scaling properties and spatial organization of snow depth fields in sub-alpine forest and alpine tundra. *Hydrological Processes*, *23*(11), 1575–1590. https://doi.org/10.1002/hyp.7270

Ullrich, A., & Pfennigbauer, C. (2011). Echo digitization and waveform analysis in airborne and Terrestrial Laser Scanning. *Photogrammetric Week*, 217–228. Retrieved from. http://www.ifp.uni-stuttgart.de/publications/phowo11/220Ullrich.pdf

Wayand, N. E., Marsh, C. B., Shea, J. M., & Pomeroy, J. W. (2018). Globally scalable alpine snow metrics. *Remote Sensing of Environment*, *213*(May), 61–72. https://doi.org/10.1016/j.rse.2018.05.012

Zheng, Z., Kirchner, P. B., & Bales, R. C. (2016). Topographic and vegetation effects on snow accumulation in the southern Sierra Nevada: A statistical summary from lidar data. *Cryosphere*, *10*(1), 257–269. https://doi.org/10.5194/tc-10-257-2016